EFFICIENT OPTIMIZATION OF HIGH-PERFORMANCE CONTOURED BEAM REFLECTARRAYS WITH REUSABLE SURFACE SHAPE FOR MULTIPLE COVERAGES

Min Zhou[1], Oscar Borries[1], Erik Jørgensen[1], Stig B. Sørensen[1], Rolf Jørgensen[1], Massimiliano Simeoni[2], and Giovanni Toso[2]

[1]*TICRA, Copenhagen, Denmark*
[2]*ESA-ESTEC, Noordwijk, The Netherlands*

ABSTRACT

This paper describes the design of high-performance contoured beam reflectarrays using a direct optimization technique with an improved optimization engine. In Ku-band, curved reflectarrays allow the reuse of a standard mold for multiple missions and thereby reduce cost and delivery time compared to shaped reflectors. To demonstrate this, two 1.2 m curved Tx-Rx contoured beam reflectarrays with the same curved surface have been designed, and by changing the reflectarray elements layout, two different coverages can be generated while maintaining performance that is comparable to that of a shaped reflector. In C-band, a deployable multi-faceted reflectarray can be an alternative solution to generate contoured beams where aperture sizes >3 m are needed. To demonstrate this, a 4.5 m multi-faceted contoured beam reflectarray has been designed to operate in a 20% bandwidth and dual-circular polarization.

Key words: Reflectarray, optimization, contoured beam, satellite application.

1. INTRODUCTION

Recently, the European Space Agency (ESA) has funded several activities to promote the use of printed reflectarrays for satellite applications with particular emphasis on contoured beam missions [1, 2]. Although showing promising results, the use of reflectarrays in the commercial telecommunication antenna segment has up until now been limited and the shaped reflector technology is still the preferred choice for most missions. This is presumably due to two reasons: inferior bandwidth performance compared to reflectors, and the lack of a reliable and commercially available design tool for reflectarrays.

To enhance the bandwidth performance of printed reflectarrays, the use of a reflectarray with elements printed on a doubly curved surface has been suggested [3]. Such a doubly curved structure has several distinct advantages compared to planar reflectarrays. Most importantly, the spatial phase delay issue is reduced, allowing performance comparable to that of an equivalently sized shaped reflector. Furthermore, a curved reflectarray enables the possibility of reusing the same mold for multiple coverages, thus reducing manufacturing costs and development time compared to shaped reflectors. Although considered before [4, 5], the use of the curved reflectarrays is relatively new and is the subject of an on-going ESA ARTES 5.1 activity. For very large apertures (>3m) where curved reflectarrays (and solid shaped reflectors) are not viable solutions, the use of a multi-faceted deployable reflectarray is more appropriate due to the available heritage on the deployment of multi-faceted solar panels [6].

For the design of contoured beam reflectarrays, the conventional design approach is based on a phase-only synthesis approach [7]. However, recent work has shown that the use of a direct optimization technique where all array elements are optimized simultaneously can provide designs with superior performance [8]. For electrically large reflectarrays consisting of many array elements, the number of optimization variables may be too large for the current direct optimization implementation. In an on-going ESA ARTES 5.2 activity, a large-scale optimization algorithm has been be implemented, reducing the optimization time and storage requirements.

In this work, the newly developed large-scale optimization algorithm is applied to design curved/multi-faceted contoured beam reflectarrays in both C-band and Ku-band. Representable results will be presented to highlight the potential of contoured beam reflectarrays.

2. OPTIMIZATION ALGORITHM

The optimization used to design the contoured beam reflectarrays is based on the direct optimization technique (DOT) presented in [9]. The analysis method is based on a spectral domain method of moments assuming local periodicity and the optimization engine is based on a gradient non-linear minimax optimization algorithm. The DOT can be applied on both planar [8], multi-faceted [10], and curved reflectarrays [5] and the reader is referred to these references for more detailed description of the direct optimization technique.

The general framework of the optimization algorithm used in the DOT is taken from the seminal work by Hald [11], which has been succesfully applied in TICRA's software POS for decades. However, the existing algorithm is not well suited for solving the large problems that arise in the direct optimization of all array elements in an electrically large reflectarray where the number of optimization variables can exceed tens of thousands. Consequently, the existing algorithm has been improved and a brief description is provided in the following.

The algorithm solves the minimax problem

$$\min_{\overline{X}}. \quad F(\overline{X}) = \max\left(F_1(\overline{X}), F_2(\overline{X}), \ldots, F_m(\overline{X})\right), \tag{1a}$$

$$\text{s.t.} \quad \overline{\overline{A}}\,\overline{X} \leq \overline{B} \tag{1b}$$

The general framework of the algorithm by Hald [11] is shown in pseudocode in Algorithm 1. The framework is based on the realization that the function value will at a given point $\tilde{\overline{X}}$ be governed by a set of active functions $\mathcal{M}$ where $\left\{F_i(\tilde{\overline{X}}) = F(\tilde{\overline{X}}) | \forall i \in \mathcal{M}\right\}$, and similarly for the active constraints. Thus, by applying the minimization theorem of [12], we can find the steepest descent feasible direction by only considering the active functions, a significant reduction in computational overhead compared to general purpose non-linear minimization algorithms.

Algorithm 1 Pseudocode for the min-max algorithm by Hald [11].

```
Initialize values at initial point X̄.
for k = 1,max_iterations do
    Find direction ΔX̄ and step length α ≤ α_max
    Evaluate T = F(X̄ + αΔX̄)
    Depending on T and F(X̄), update α_max and X̄.
end for
```

However, for the implementation of the algorithm, several mathematical components are needed, and the details in the implementation of these components will govern the final performance of the algorithm.

In the original implementation by Hald, a direct factorization of the initial active set matrix was used to take the initial step in a linear model of the trust region around the current point, and then rank-1 updates of the factorization was performed to include and remove functions and constraints from the active set as the algorithm stepped towards the edge of the trust region. While this approach yields very high accuracy, it suffers three problems. First, it is computationally quite intensive. Second, it is inherently serial, and thus cannot be adapted to modern parallel computing architectures. Third, it requires sophisticated control structures to prevent cycling of the active set, particularly as the step begins to reach the edge of the trust region.

To avoid this, we reformulated the step-finding algorithm to apply modern techniques from convex optimization, including all active functions and constraints simultaneously, as well as those that are close to becoming active. This is faster, can be parallelized by parallelizing the convex solver, and avoids the risk of cycling. In practice, the algorithm is orders of magnitude faster than the original implementation by Hald, particularly as the number of unknowns N and the number of functions m increase beyond, say, a thousand.

Another problem with the old implementation was the use of an exact linesearch which, while accurate, would favor a high number of very short steps. For the new implementation, we need to take a small number of large steps, simultaneously activating a large number of functions and constraints — while this requirement favors an inexact linesearch, our research found that this would not provide sufficient accuracy. Thus, we had to find a customized linesearch algorithm, which would allow us to apply exact linesearch in an efficient manner for a large number of newly activated functions/constraints.

Finally, the constraint matrix $\overline{\overline{A}}$ is often extremely sparse, containing at most a couple of entries per row, despite having N columns. The algorithm by Hald cannot exploit sparsity due to the use of a non sparsity-preserving factorization, and thus uses a significant amount of memory just to store $\overline{\overline{A}}$ and the factorization. In the newly developed algorithm, one only needs matrix-vector products with $\overline{\overline{A}}$ and access to the rows corresponding to active functions, and thus the sparsity is easily exploited to achieve a large reduction in memory footprint. In some cases, the reduction can be by as much as a factor of N.

3. CONTOURED BEAM REFLECTARRAYS IN KU-BAND

In Ku-band, shaped reflectors are widely used to generate contoured beams over geographical areas. However, due to its high manufacturing cost and long delivery time, cheaper solutions are of great interest. To this end, the curved reflectarray is a candidate that can reduce cost and delivery time due to the possibility of reusing an existing mold for multiple missions. To benefit from this, it is important to demonstrate that reflectarrays with the same curved surface can be used to generate different coverages while maintaining a good performance for all coverages.

In this section, we examine the performance of curved contoured beam reflectarrays with reusable surface shape for multiple coverages.

3.1. Mission Definitions

Two missions will be considered. The first mission is a South American coverage as presented in [1]. It involves a high-gain coverage in South America and an isolation coverage in Europe, see Figure 1. The antenna shall work in dual-linear polarization in both Tx (11.7-12.1 GHz) and Rx (13.75-14.25 GHz) frequency bands. For the detailed mission specifications, the reader is referred to [1].

Figure 1. The South American and European coverages from [1].

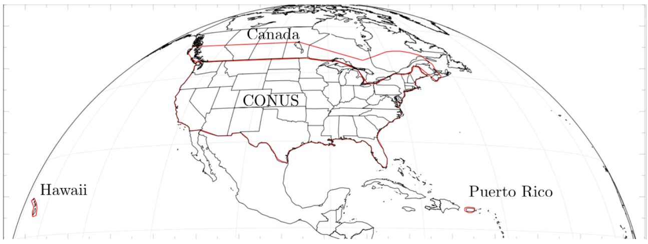

Figure 2. Continental United States coverage from [2].

The second mission is the coverage presented in [2] and shown in Figure 2. It covers CONUS/Canada with two separate regions over Puerto Rico and Hawaii. For simplicity, we select the same frequency bands as the first mission, namely Tx (11.7-12.1 GHz) and Rx (13.75-14.25 GHz). The antenna must operate in dual-linear polarization with a minimum directivity of 28.4 dBi and a minimum cross-polar discrimination (XPD) of 30.0 dB over all the coverages.

3.2. Reflectarray Configuration

The configuration considered for the reflectarray designs is shown in Figure 3. The reflectarray has a circular projected aperture size of 1.2 m seen from the main beam direction which is given by the $(x_{\mathrm{sta}}, y_{\mathrm{sta}}, z_{\mathrm{sta}})$ coordinate system. The reflectarray coodinate system is defined such that the specular reflection from the surface is aligned with the z_{sta}-axis. As feed, a Gaussian beam model is used.

As stated in [5], it is important that the curvature of the reflectarray surface is selected such that the configuration (without the presence of the array elements) provides a defocused beam that is similar to the required cover-

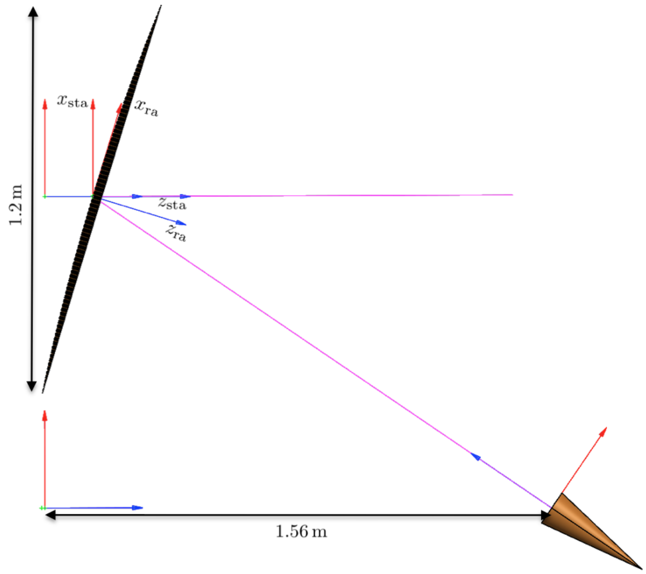

Figure 3. Offset configuration with a rotationally symmetrical parabolic surface defined wrt. the $(x_{\mathrm{ra}}, y_{\mathrm{ra}}, z_{\mathrm{ra}})$ coordinate system. By adjusting the focal length of this surface, different degrees of defocusing can be achieved.

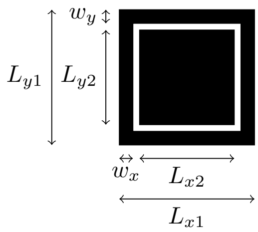

Figure 4. Rectangular loop/patch combination element.

age area. Then the detailed coverage shape is achieved by optimizing the array elements. The defocusing can be achieved in several ways. In our case, the defocused surface is described by a rotationally symmetrical paraboloid. This rotationally symmetrical parabolic surface is defined wrt. the $(x_{\mathrm{ra}}, y_{\mathrm{ra}}, z_{\mathrm{ra}})$ coordinate system. By adjusting the focal length of this parabolic surface, different degrees of defocusing can be achieved. In this work, the focal length of this surface is selected to 3.0 meters. The idea is to use this configuration (same surface, same f/D, same dimension, and same feed) and generate the coverages for mission 1 and 2 by simply changing the reflectarray elements layout.

As array element, the rectangular loop/patch combination element (see Figure 4) which is used in [8] is considered. As optimization variables, L_{x1} and L_{y1} are included whereas the other parameters are fixed with respect to that used in [8]. The number of array elements in the curved reflectarrays is 6,437 resulting in a total of 12,874 optimization variables.

3.3. Numerical Results

By applying the direct optimization technique two reflectarrays that use exactly the same surface, f/D, dimension, and feed have been designed. Using the old minimax algorithm, the optimization time to arrive at the optimized designs was more than 24 hours per design on a standard laptop computer. With the new algorithm, the optimization can be done in less than a hour which is a substantial improvement.

The first reflectarray is optimized for mission 1 (South America) and it fulfills all the requirements in the entire Tx-Rx band for both linear polarizations with a margin of 0.53 dB. The second reflectarray is optimized for mission 2 (CONUS) and similarly, it fulfills all the requirements with a margin of 0.90 dB. The radiation patterns, co-polar directivity and XPD, of the optimized reflectarrays at 14.25 GHz in V-polarization are shown in Figure 5 and Figure 6. Similar results are observed for the H-polarization and the other frequencies and are therefore not shown.

For comparison purposes, two shaped reflectors with identical dimensions and f/D of the reflectarrays have been designed. They are optimised to fulfill the requirements of mission 1 and 2, one reflector for each mission. For mission 1, the shaped reflector fulfills the coverage specifications with a margin of 0.68 dB, and for mission 2 the shaped reflector fulfills the requirements with a margin of 0.95 dB. Thus, compared to the curved reflectarrays, the shaped reflectors are slightly superior in performance, by between 0.05-0.15 dB. However, there are a number of factors that should be mentioned to better understand the differences between the shaped reflectors and the curved reflectarrays.

First, the surface curvature (focal length of 3 m) of the reflectarrays is selected as a compromise for the two coverages based on a fixed f/D. A different value of the focal length for the surface can actually provide better performance for one of the missions. For instance, for mission 2, the use of a parabolic surface with a focal length of 2.7 m can actually provide a reflectarray design that fulfills the requirements with a margin of 0.96 dB which is identical to that of the shaped reflector. However, for mission 1, the performance degrades using this surface. Similarly, by increasing the focal length of the surface, the performance for mission 1 can be enhanced but at the cost of a degradation for mission 2. Thus, there will always be a trade-off depending on the coverage. This can be alleviated by moving the position of the feed for each coverage. By adjusting the distance between the feed and the surface, the defocusing can be regulated to better match the shape of the specified coverage and hence improve the performance.

Second, the direction of the main-beam towards the coverage can be adjusted by tilting the surface with respect to the feed. Depending on the coverage shape this may also have an impact on the reflectarray performance, in particular for asymmetric coverages such as the one for mission 1. The tilt of the surface is not considered for the curved reflectarrays, but for the shaped reflectors, this is automatically adjusted during the optimization process in POS.

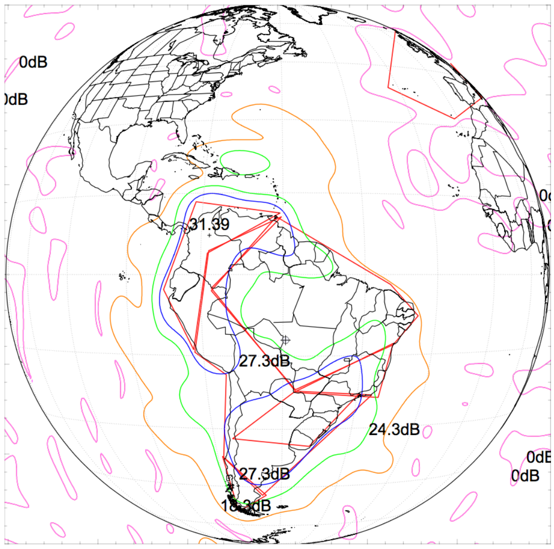

(a) Co-polar directivity [dBi]

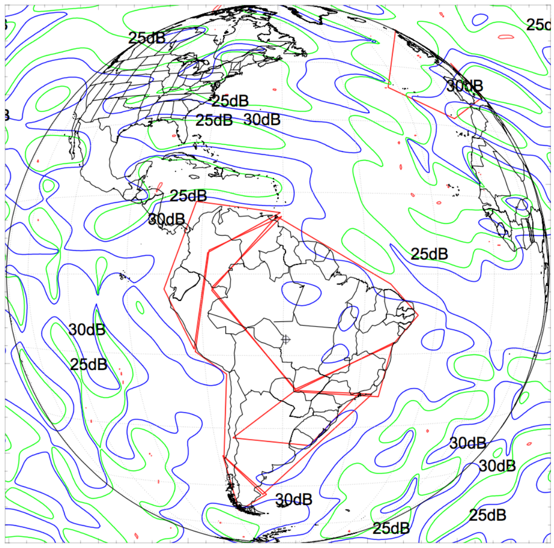

(b) XPD [dB]

Figure 5. Simulated radiation patterns of the optimized curved reflectarray for mission 1 at 14.25 GHz in V-polarization.

Finally, as already mentioned, the coverage for mission 1 is rather asymmetric, thus a rotationally symmetrical parabolic surface may not be the best choice for this mission. The coverage for mission 2 on the other hand is more symmetric and a rotationally symmetrical parabolic surface is a good candidate as reflectarray surface. This also explains why the performances between the reflectarrays and the shaped reflector are more comparable for mission 2 than the designs for mission 1.

From a RF point of view, the results presented here are very encouraging and suggests that a curved reflectarray

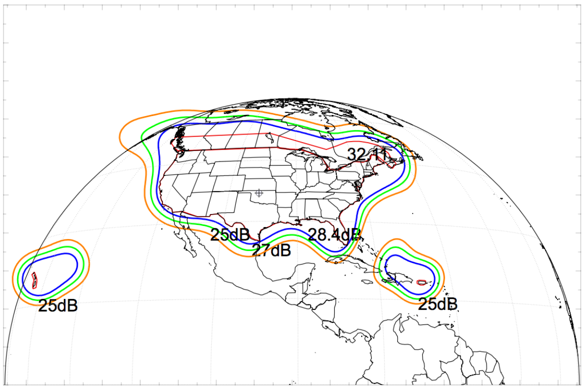

(a) Co-polar directivity [dBi]

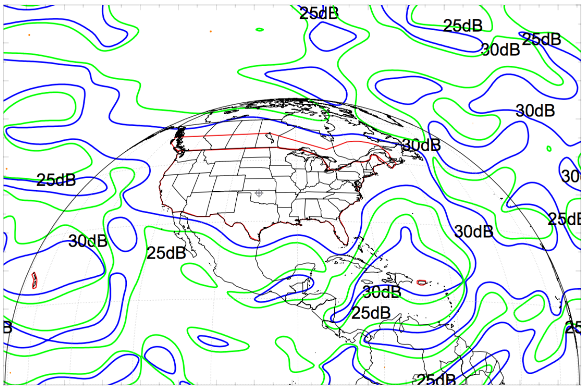

(b) XPD [dB]

Figure 6. Simulated radiation patterns of the optimized curved reflectarray for mission 2, at 14.25 GHz in V-polarization.

may be able to replace shaped reflectors for telecommunication applications. However, from a manufacturing point of view, there are still some challenges. The proposed designs are based on single layer substrate but a sandwich structure may be required for space applications. A sandwich structure implies the use of multiple substrate layers which will increase losses. Additionally, the array elements need to be etched on a doubly curved surface and a non-conventional manufacturing approach is needed. TICRA is working with experts in this area with the aim to manufacture a breadboard to demonstrate its feasibility.

4. CONTOURED BEAM REFLECTARRAYS IN C-BAND

Solid reflectors (hence also curved reflectarrays) are usually limited to an aperture size of less than 3 m and this is one of the major limitations for telecom satellites operating in lower frequencies such as L, S, and C-band. With the recent improvements in mesh reflector technology, it is now possible to have aperture sizes >3 m. However, the mesh reflector antennas, currently based on a parabolic surface, can only generate pencil beams unless a complex focal array is implemented to produce a contoured beam pattern.

A multi-faceted reflectarray is an interesting alternative and circumvents some of the issues associated with mesh reflector antennas, e.g., unwanted generation of grating lobes. With the existing heritage on the deployment of multi-faceted solar panels, the deployment of a multi-faceted reflectarray seems feasible [6] and makes the multi-faceted reflectarray a viable solution in lower frequency bands.

In this section, we present the design of a multi-faceted reflectarray in C-band to demonstrate its potential use.

4.1. Coverage Definitions

For simplicity, we consider the same CONUS coverage as before (Figure 2) with the same co- and cross-polar requirements. However, contrary to before, the multi-faceted reflectarray needs to operate in dual-circular polarization and the frequency band is between 3.9-4.75 GHz which yields a bandwidth of approximately 20%.

4.2. Reflectarray Configuration

The multi-faceted reflectarray has an aperture size of 4.5 m and consists of 9 panels as shown in Figure 7. Similar to the design of curved reflectarrays, the panels should imitate a curved surface that provides a defocused beam for the same reasons as for the curved reflectarrays. Consequently, the 9 panels are defined to imitate a rotationally symmetrical parabolic surface similar to the one considered for the aforementioned curved reflectarrays. This is simply done by tilting the panels with respect to each other.

The rectangular loop/patch combination element is also used for this reflectarray, however, the dimensions and substrate have been scaled to operate at the lower frequencies. The number of array elements in the multi-faceted reflectarray is 10,440 resulting in a total of 20,880 optimization variables. Again, a Gaussian beam model is used as feed.

4.3. Numerical Results

The direct optimization technique has been used to optimize the multi-faceted reflectarray. With the new optimization algorithm, the design was done on a laptop computer and the optimization took approximately one hour.

One of the most challenging aspects in the design of contoured beam reflectarrays is to fulfill the coverage requirements in a wide bandwidth, in this case approximately 20%. However, with the direct optimization technique in conjunction with the multi-faceted structure, the optimized multi-faceted reflectarray fulfills the requirements in the entire frequency band for both polarizations.

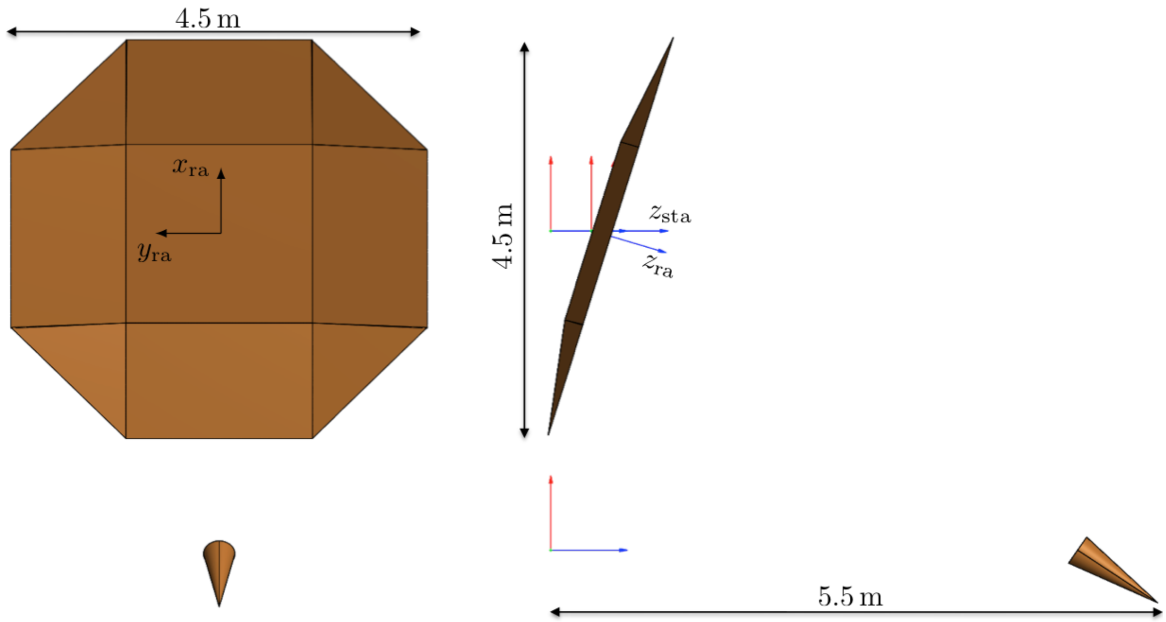

Figure 7. Offset multi-faceted reflectarray configuration consisting of 9 panels.

In Figure 8 and Figure 9, the radiation patterns of the optimized multi-faceted reflectarray for right-hand circular polarization (RHCP) at the lowest frequency (3.9 GHz) and the highest frequency (4.75 GHz), respectively, are shown. It is seen that the reflectarray radiates high-gain beams over the CONUS, Canada, Hawaii, and Puerto Rico with a XPD above 30 dB over all high-gain regions. Similar patterns are also observed for the frequencies in between and for left-hand circular polarization (LHCP).

Using the same multi-faceted configuration, one could easily reoptimize the array elements such that a completely different coverage is generated by the antenna. This implies that there will be a trade-off depending on the coverage, just like in the case of curved reflectarrays. However, the panels can be easily adjusted by tilting the panels differently and thereby imitating a different surface. But most importantly, the multi-faceted reflectarray provides a solution to generate contoured beams at the lower frequencies where aperture sizes >3 m are needed.

5. CONCLUSIONS

TICRA's direct optimization technique for printed reflectarrays have been updated with a new optimization engine. With the new enhanced optimization engine, the optimization time can be reduced by several orders of magnitudes hence allowing the design of a high-performance contoured reflectarray in less than a hour. To demonstrate this, contoured beams in Ku- and C-band have been designed.

In Ku-band, two 1.2 m curved Tx-Rx contoured beam reflectarrays have been designed. These two reflectarrays use the same curved surface and by simply changing the reflectarray elements layout, two completely different coverages can be produced while maintaining a perfor-

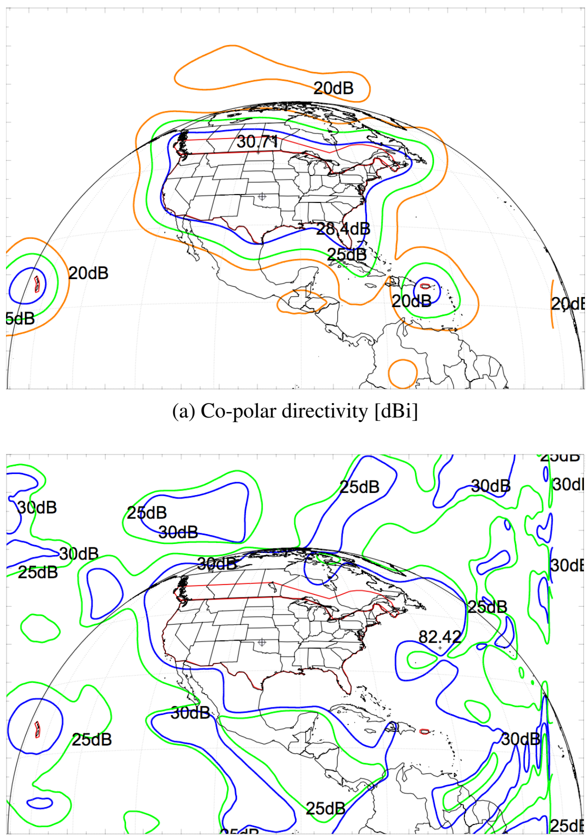

(a) Co-polar directivity [dBi]

(b) XPD [dB]

Figure 8. Simulated radiation patterns of the optimized multi-faceted reflectarray at 3.9 GHz in RHCP.

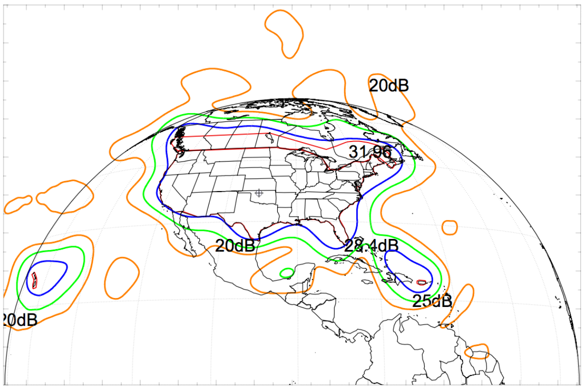

(a) Co-polar directivity [dBi]

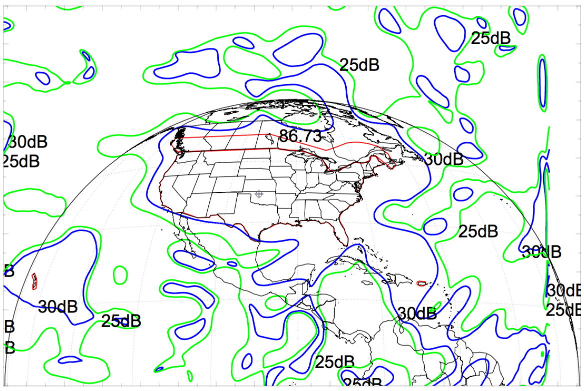

(b) XPD [dB]

Figure 9. Simulated radiation patterns of the optimized multi-faceted reflectarray at 4.75 GHz in RHCP.

mance that is comparable with that of the shaped reflector in a bandwidth of 20%. This highlights the advantage of curved reflectarrays over shaped reflectors that a standard mold can be used for multiple missions hence reducing cost and schedule.

In C-band, a 4.5 m multi-faceted contoured beam reflectarray has been designed. This reflectarray operates in a 20% bandwidth in dual-circular polarization and demonstrates that multi-faceted contoured beam reflectarrays are viable solutions to generate contoured beams in lower frequencies where aperture sizes >3 m are needed.

ACKNOWLEDGMENTS

This work is supported by the European Space Agency (ESA) within the ESTEC Contract No. 4000115345/15/NL/ND and ESTEC Contract No. 4000116990/16/NL/US.

REFERENCES

[1] J. A. Encinar, M. Arrebola, L. D. L. Fuente, and G. Toso, "A transmit-receive reflectarray antenna for direct broadcast satellite applications," *IEEE Trans. Antennas Propag.*, vol. 59, no. 9, pp. 3255–3264, 2011.

[2] H. Legay, D. Bresciani, R. Chiniard, E. Girard, G. Caille, E. Labiole, and R. Gillard, "Demonstration model of a reflectarray for telecomminca-tion antenna, Final report," Thales Alenia Space, Toulouse, France, Tech. Rep., March 2012.

[3] M. E. Cooley, T. J. Chwalek, and P. Ramanujam, "Method for improving pattern bandwidth of shaped reflectarrays," *US Patent 6,031,506*, February 2000.

[4] J. A. Encinar, M. Arrebola, and G. Toso, "A parabolic reflectarray for a bandwidth improved contoured beam coverage," in *Proc. EuCAP*, Edinburgh, UK, 2007.

[5] M. Zhou, S. B. Sørensen, O. Borries, and E. Jørgensen, "Analysis and optimization of a curved transmit-receive contoured beam reflectarray," in *Proc. EuCAP*, Lisbon, Portugal, 2015.

[6] R. Chiniard, L. Schreider, N. Girault, S. Vezain, E. Labiole, G. Caille, Y. Baudasse, H. Legay, and D. Bresciani, "Study of a very large reflect array antenna built with unfoldable panels for L to C missions," in *Proc. ESA Workshop on Large Deployable Antennas*, Noordwijk, The Netherlands, 2012.

[7] D. M. Pozar, S. D. Targonski, and H. D. Syrigos, "Design of millimeter wave microstrip reflectarrays," *IEEE Trans. Antennas Propag.*, vol. 45, no. 2, pp. 287–296, 1997.

[8] M. Zhou, O. Borries, and E. Jørgensen, "Design and optimization of a single-layer planar transmit-receive contoured beam reflectarray with enhanced performance," *IEEE Trans. Antennas Propag.*, vol. 63, no. 3, pp. 1247–1254, 2015.

[9] M. Zhou, S. B. Sørensen, O. S. Kim, E. Jørgensen, P. Meincke, and O. Breinbjerg, "Direct optimization of printed reflectarrays for contoured beam satellite antenna applications," *IEEE Trans. Antennas Propag.*, vol. 61, no. 4, pp. 1995–2004, 2013.

[10] M. Zhou, S. B. Sørensen, P. Meincke, and E. Jørgensen, "Design and optimization of multi-faceted reflectarrays for satellite applications," in *Proc. EuCAP*, The Hague, The Netherlands, 2014.

[11] J. Hald, "Two stage algorithms for linearly constrained minimax optimization," Ph.D. dissertation, Technical University of Denmark, 1984.

[12] V. F. Dem'yanov and V. N. Malozemov, *Introduction to minimax*, ser. Dover books on advanced mathematics. Dover Publications, 1990.